OPEN

Neuropsychopharmacology (2013) 38, 1409–1425

www.neuropsychopharmacology.org

Deficiency of Schnurri-2, an MHC Enhancer Binding Protein, Induces Mild Chronic Inflammation in the Brain and Confers Molecular, Neuronal, and Behavioral Phenotypes Related to Schizophrenia

Keizo Takao[1,2,3], Katsunori Kobayashi[3,4], Hideo Hagihara[1,3], Koji Ohira[1,3], Hirotaka Shoji[1,3], Satoko Hattori[1,3], Hisatsugu Koshimizu[1,3], Juzoh Umemori[1,3], Keiko Toyama[1,3], Hironori K Nakamura[1,3], Mahomi Kuroiwa[3,5], Jun Maeda[6], Kimie Atsuzawa[7], Kayoko Esaki[8], Shun Yamaguchi[9,10], Shigeki Furuya[8], Tsuyoshi Takagi[11,12], Noah M Walton[13], Nobuhiro Hayashi[14], Hidenori Suzuki[3,4], Makoto Higuchi[6], Nobuteru Usuda[7], Tetsuya Suhara[6], Akinori Nishi[3,5], Mitsuyuki Matsumoto[13], Shunsuke Ishii[10] and Tsuyoshi Miyakawa*[,1,2,3]

[1]Division of Systems Medical Science, Institute for Comprehensive Medical Science, Fujita Health University, Toyoake, Japan; [2]Section of Behavior Patterns, Center for Genetic Analysis of Behavior, National Institute for Physiological Sciences, Okazaki, Japan; [3]Japan Science and Technology Agency, CREST, Kawaguchi, Japan; [4]Department of Pharmacology, Graduate School of Medicine, Nippon Medical School, Tokyo, Japan; [5]Department of Pharmacology, Kurume University School of Medicine, Kurume, Japan; [6]Molecular Neuroimaging Program, Molecular Imaging Center, National Institute of Radiological Sciences, Chiba, Japan; [7]Department of Anatomy II, Fujita Health University School of Medicine, Toyoake, Japan; [8]Department of Bioscience and Biotechnology, Graduate School of Bioresource and Bioenvironmental Sciences, Kyushu University, Fukuoka, Japan; [9]Division of Morphological Neuroscience, Gifu University Graduate School of Medicine, Gifu, Japan; [10]Japan Science and Technology Agency, PRESTO, Kawaguchi, Japan; [11]RIKEN Tsukuba Institute, Tsukuba, Japan; [12]Institute for Developmental Research, Aichi Human Service Center, Kasugai, Japan; [13]Astellas Research Institute of America LLC, Skokie, IL, USA; [14]Graduate School of Bioscience and Biotechnology, Tokyo Institute of Technology, Tokyo, Japan

Schnurri-2 (Shn-2), an nuclear factor-κB site-binding protein, tightly binds to the enhancers of major histocompatibility complex class I genes and inflammatory cytokines, which have been shown to harbor common variant single-nucleotide polymorphisms associated with schizophrenia. Although genes related to immunity are implicated in schizophrenia, there has been no study showing that their mutation or knockout (KO) results in schizophrenia. Here, we show that Shn-2 KO mice have behavioral abnormalities that resemble those of schizophrenics. The mutant brain demonstrated multiple schizophrenia-related phenotypes, including transcriptome/proteome changes similar to those of postmortem schizophrenia patients, decreased parvalbumin and GAD67 levels, increased theta power on electroencephalograms, and a thinner cortex. Dentate gyrus granule cells failed to mature in mutants, a previously proposed endophenotype of schizophrenia. Shn-2 KO mice also exhibited mild chronic inflammation of the brain, as evidenced by increased inflammation markers (including GFAP and NADH/NADPH oxidase p22 phox), and genome-wide gene expression patterns similar to various inflammatory conditions. Chronic administration of anti-inflammatory drugs reduced hippocampal GFAP expression, and reversed deficits in working memory and nest-building behaviors in Shn-2 KO mice. These results suggest that genetically induced changes in immune system can be a predisposing factor in schizophrenia.
Neuropsychopharmacology (2013) **38,** 1409–1425; doi:10.1038/npp.2013.38; published online 6 March 2013

Keywords: animal models; dentate gyrus; endophenotype; inflammation; mood/anxiety/stress disorders; psychiatry & behavioral sciences; schizophrenia/antipsychotics

INTRODUCTION

Elucidating the neural and genetic basis of schizophrenia and other psychiatric disorders remains difficult, in part because psychiatric phenotypes in human patients are largely dependent on subjective clinical evaluation criteria that lack quantifiable biological indicators. The biological heterogeneity of schizophrenia patients has particularly hindered the

*Correspondence: Professor T Miyakawa, Division of Systems Medical Science, Institute for Comprehensive Medical Science, Fujita Health University, 1-98, Dengakugakubo, Kutsukake-cho, Toyoake 470-1192, Japan. Tel: +81 562 93 9375, Fax: +81 562 92 5328,
E-mail: miyakawa@fujita-hu.ac.jp
Received 11 December 2012; accepted 2 January 2013; accepted article preview online 6 February 2013

identification of genetic risk factors (Braff *et al*, 2007). Thus, the development of animal models with homogenous backgrounds is imperative for investigating genetic contributions to schizophrenia. For the past decade, we have sought to identify rodent models of neuropsychiatric disorders, including schizophrenia, by analyzing genetically engineered mice with a comprehensive behavioral test battery that covers many distinct behavioral domains, from simple sensorimotor functions to cognition-intensive functions like learning and memory (Miyakawa *et al*, 2003; Powell and Miyakawa, 2006; Yamasaki *et al*, 2008). To date, we have screened >140 mutant mouse strains using the same protocol and identified several strains with behavioral phenotypes that resemble symptoms in human schizophrenia patients (Takao *et al*, 2008; Yamasaki *et al*, 2008).

Schnurri-2 (Shn-2; also called major histocompatibility complex (MHC)-binding protein 2 (MBP-2), Hivep2 or Mibp1) was originally identified as a nuclear factor-κB (NF-κB) site-binding protein that tightly binds to the enhancers of MHC genes in the MHC regions of chromosome 6 (Fukuda *et al*, 2002). Recent genome-wide association studies identified a number of single-nucleotide polymorphisms (SNPs) in the MHC region associated with schizophrenia (Purcell *et al*, 2009; Shi *et al*, 2009, 2011; Stefansson *et al*, 2009; Yue *et al*, 2011). MHC class I proteins coded in this region have been reported to play a critical role in neural development and plasticity (Shatz, 2009). Genes in MHC regions often contain NF-κB-binding sequences in their promoter regions. Shn-2 constitutively binds NF-κB-binding site to suppress NF-κB-dependent gene expression (Kumar *et al*, 2004), including tumor necrosis factor (TNF)-α, interleukin (IL)-1β, IL-6, cyclin D1, prostaglandin-endoperoxidase synthase 2 (PTGS2, also called COX2), NADH/NADPH oxidase p22 phox, and vimentin. To induce an immune response, Shn-2 detaches from the NF-κB-binding site, allowing the transcription of NF-κB target genes (Kimura *et al*, 2005, 2007). Accordingly, Shn-2 KO mice demonstrate constitutive NF-κB activation in CD4+ T cells (Kimura *et al*, 2007). Shn-2 expression is also reported in several brain regions including hippocampus, cortex, and cerebellum (Fukuda *et al*, 2002). We previously reported that Shn-2 KO mice exhibited hyperactivity (Takagi *et al*, 2006), suggesting the functional significance of Shn-2 in the brain.

As a course of our large-scale screening to identify animal models of psychiatric disorders, Shn-2 KO mice were subjected to a comprehensive behavioral test battery. Shn-2 KO mice displayed behavioral alterations and cognitive impairments resembling those of schizophrenia. We observed significant similarities in transcriptome/proteome changes between Shn-2 KO mouse brain and postmortem brains of human schizophrenia patients. Granule cells of the dentate gyrus (DG) also failed to mature in Shn-2 KO mice, a previously proposed candidate endophenotype of the disease observed in at least one additional mouse model of schizophrenia and its related phenotypes (Yamasaki *et al*, 2008). Finally, Shn-2 KO mice demonstrated mild, widespread brain inflammation characterized by the upregulation of NF-κB-responsive genes and activation of astrocytes. Our results demonstrate that Shn-2 KO mice serve as an animal model of schizophrenia with good face and concept validity. The present study also suggests that immune system changes induced by genetic factors may contribute to the pathophysiology of schizophrenia.

MATERIALS AND METHODS

A detailed description of the Materials and Methods is provided in the Supplementary Text.

Animals and Experimental Design

Shn-2 KO mice and wild-type control littermates were obtained by breeding heterozygotes with a C57BL/6J background and those with a BALB/cA background. All behavioral tests were carried out with mice that were at least 9 weeks old at the start of testing. Raw data from the behavioral tests, the date on which each experiment was performed, and the age of the mice at the time of the experiment are shown in the mouse phenotype database (http://www.mouse-phenotype.org/). Mice were group-housed (2–4 mice per cage) in a room with a 12-h light/dark cycle (lights on at 0700 hours) with access to food and water *ad libitum*. The room temperature was kept at $23 \pm 2\,^{\circ}C$. Behavioral testing was performed between 0900 and 1800 hours. After the tests, all apparatus were cleaned with diluted sodium hypochlorite solution to prevent bias due to olfactory cues. Eighteen independent groups of mice were prepared for behavioral tests. The number of animals used for each of the tests is shown in the corresponding figures and tables. All behavioral tests were separated from each other by at least 1 day. All behavioral testing procedures were approved by the Animal Research Committee, Graduate School of Medicine, Kyoto University, Fujita Health University and National Institute for Physiological Sciences.

Gene Expression Analysis

RNA was isolated by using the TRIzol method (Invitrogen, Carlsbad, CA) from mouse brains, followed by purification, using RNeasy columns (Qiagen, Valencia, CA). GeneChip analyses were conducted as previously described (Yamasaki *et al*, 2008). cDNA was synthesized from the total RNA, and *in vitro* transcription reaction was then performed on biotin-labeled RNA that was made from the cDNA. Labeled RNA was hybridized with Mouse Genome 430 2.0 Array (Affymetrix, Santa Clara, CA) containing 45101 probe sets, and washed according to the manufacturer's recommendations. The hybridized probe array was then stained with streptavidin-conjugated phycoerythrin, and each GeneChip was scanned by an Affymetrix GeneChip Scanner 3000 (GCS3000).

Public microarray data sets were queried using NextBio, a database of microarray results (accessed on 14 May 2011). NextBio is a repository of analyzed microarray data sets that allows the investigator to search results and the expression profiles of publicly available microarray data sets. Gene overlaps were examined using Running Fisher test.

Immunohistochemistry

Mice were deeply anesthetized with chloral hydrate (245 mg/kg, i.p.) and transcardially perfused with 4% paraformaldehyde in 0.1 M phosphate buffer, pH 7.4. The brains were

dissected, immersed overnight in the same fixative, and transferred to 30% sucrose in PBS for at least 3 days for cryoprotection. The brain samples were mounted in Tissue-Tek (Miles, Elkhart, IN), frozen, and cut into 50-μm-thick coronal sections using a microtome (CM1850, Leica Microsystems, Wetzlar, Germany). The sections were washed with Tris-buffered saline containing Tween 20 (pH 7.4). For immunostaining, the cryostat sections were incubated at 4 °C for 18 h with the following primary antibodies: calbindin (mouse monoclonal antibody 300 and rabbit polyclonal antibody D-28k; Swant, Bellinzona, Switzerland), calretinin (mouse monoclonal antibody 6B3 and rabbit polyclonal antibody 7699/4; Swant), GAD67 (MAB5406; Millipore, Temecula, CA), mouse anti-CNPase monoclonal (C5922; Sigma-Aldrich, St Louis, MO), GFAP (G9269; Sigma-Aldrich), p22 phox (sc-20781; Santa Cruz Biotechnology, San Diego, CA), goat polyclonal antibody for parvalbumin (PVG-214; Swant). To detect antigen localization, the sections were incubated at 4 °C for 2 h with Alexa Fluor (488 or 594)-conjugated goat anti-mouse IgM or IgG antibody (1 : 400 dilution; Invitrogen) and/or Alexa Fluor (488 or 594)-conjugated goat anti-rabbit IgG antibody (1 : 400 dilution; Invitrogen). Fluorescent signals were detected using a confocal laser-scanning microscope (LSM 700, Zeiss, Oberkochen, Germany) or a fluorescence microscope (Axioplan-2, Zeiss).

Two-Dimensional Fluorescence Difference Gel Electrophoresis (2D-DIGE)

The DG was dissected out (Hagihara *et al*, 2009), frozen with liquid nitrogen, and stored at −80 °C until use. Twenty micrograms of each protein were dissolved in 30 mM Tris, pH 8.5 containing 2 M thiourea, 7 M urea, and 4% w/v CHAPS and minimally labeled with CyDye DIGE fluors according to the manufacturer's instructions (GE Healthcare, Little Chalfont, UK). In brief, the dyes were added to the protein extract (8 pmol/μg protein). Internal pools were generated by combining equal amounts of all samples and labeled with Cy2. After vortexing, centrifugation, and incubation (30 min in the dark at 4 °C), 10 mM L-lysine (Sigma-Aldrich) was added to stop the reaction (10 min in the dark at 4 °C). Equal amounts of Cy2-, Cy3-, and Cy5-labeled protein samples were mixed, and rehydration buffer (GE Healthcare) was added to a final volume of 125 μl. Isoelectric focusing was performed using Immobiline DryStrip (pH 3–10, 7 cm, GE Healthcare) and an Ettan IPGphorIII (GE Healthcare) at 300 V for 200 V · h, 1 kV for 300 V · h, and 5 kV for 6 kV · h. After the reduction and alkylation of disulfide bonds with 10 mg/ml DTT and 25 mg/ml iodoacetamide, respectively, the second-dimension separation was run on NuPAGE gels (Invitrogen). The gels were scanned on a Typhoon 9400 imager (GE Healthcare). Excitation and emission wavelengths were chosen specifically for each dye according to the manufacturer's recommendations. Intra-gel spot detection and intra-gel matching were performed using DeCyder software (GE Healthcare). Differentially expressed protein spots were determined by pairwise comparison of the mutants with the respective control data using Student's *t*-test.

Protein Identification by Mass Spectrometry

In-gel trypsin digestion and mass spectrometry (MS) analysis were carried out essentially according to the method described previously (Kurosawa *et al*, 2009). Sypro-Ruby (Invitrogen)-stained 2D gels were used. Protein spots on the gel were excised, washed, dehydrated, added to 20 μg/μl trypsin (Promega, Fitchburg, WI) solution, and digested overnight at 37 °C. Peptide segments were extracted sequentially in 0.1% trifluoroacetic acid (TFA)/60% acetonitrile (ACN), 0.1% TFA/80% ACN, and 0.1% TFA/100% ACN. The supernatant was concentrated by centrifugal evaporator and added to 0.1% TFA/2% ACN.

The obtained peptides were separated using a nano-flow multidimensional HPLC system (Paradigm MS4; Michrom Bio Resources, Auburn, CA) and analyzed by electrospray ionization ion trap MS (LCQDECAXP; Thermo Fisher Scientific, Waltham, MA) under optimum conditions (Kurosawa *et al*, 2009). MS/MS spectra were acquired in a data-dependent mode. The resulting spectra were analyzed, and the peptide sequences were searched against a protein database (MSDB) using MASCOT software (Matrix Science, London, UK).

Image Analysis

The applications used for the behavioral studies (Image RM, Image TM, Image CSI, and Image SI) were based on the public domain NIH Image program (developed at the US National Institutes of Health and available at http://rsb.info.nih.gov/nih-image/) and ImageJ program (http://rsb.info.nih.gov/ij/), which were modified for each test (available through O'Hara & Co., Tokyo, Japan).

Statistical Analysis

Statistical analysis was conducted using StatView (SAS Institute, Cary, NC). Data were analyzed by one-way ANOVA, two-way ANOVA, or two-way repeated-measures ANOVA, unless noted otherwise. Values in tables and graphs are expressed as the mean ± s.e.m.

RESULTS

Shn-2 KO Mice Display Behavioral Abnormalities Reminiscent of Schizophrenia

Hyperactivity is one of the most common phenotypes in animal models of schizophrenia or bipolar disorder. Since Shn-2 KO mice were reported to show hyperactivity during open field testing (Takagi *et al*, 2006), we subjected them to a comprehensive behavioral test battery (Yamasaki *et al*, 2008) to further analyze the behavioral effects of Shn-2 deficiency. Shn-2 KO mice showed no obvious deficits in general health, physical characteristics, or basic sensorimotor functions compared with their wild-type littermates, apart from decreased sensitivity to pain in the hot plate test and a lower body weight (Supplementary Table 1; Supplementary Figure 1). Shn-2 KO mice displayed severe working memory deficits in the eight-arm radial maze (Figure 1a and b) and T-maze forced-alternation task (Figure 1c and d), while their performance in the T-maze

left–right discrimination task was normal (Figure 1e). In reversal learning, mutants performed even better than controls (Figure 1e). This working memory impairment is commonly found in schizophrenia patients and is referred to as a cognitive endophenotype of schizophrenia (Kalkstein *et al*, 2010). Shn-2 KO mice also showed a series of other schizophrenia-related abnormal behaviors: Prepulse inhibition (PPI), the phenomenon by which a weak prestimulus suppresses the response to a startling stimulus, is often decreased in schizophrenic patients compared with healthy controls (Swerdlow *et al*, 2006). In Shn-2 KO mice, while the amplitude of the acoustic startle response was comparable with that of wild-type controls (Figure 1f; Supplementary Figure 1a), the PPI of the acoustic startle response was markedly reduced (Figure 1g). High-dose administration of haloperidol, a typical antipsychotic, significantly improved this impairment in PPI in Shn-2 KO mice (Figure 1g).

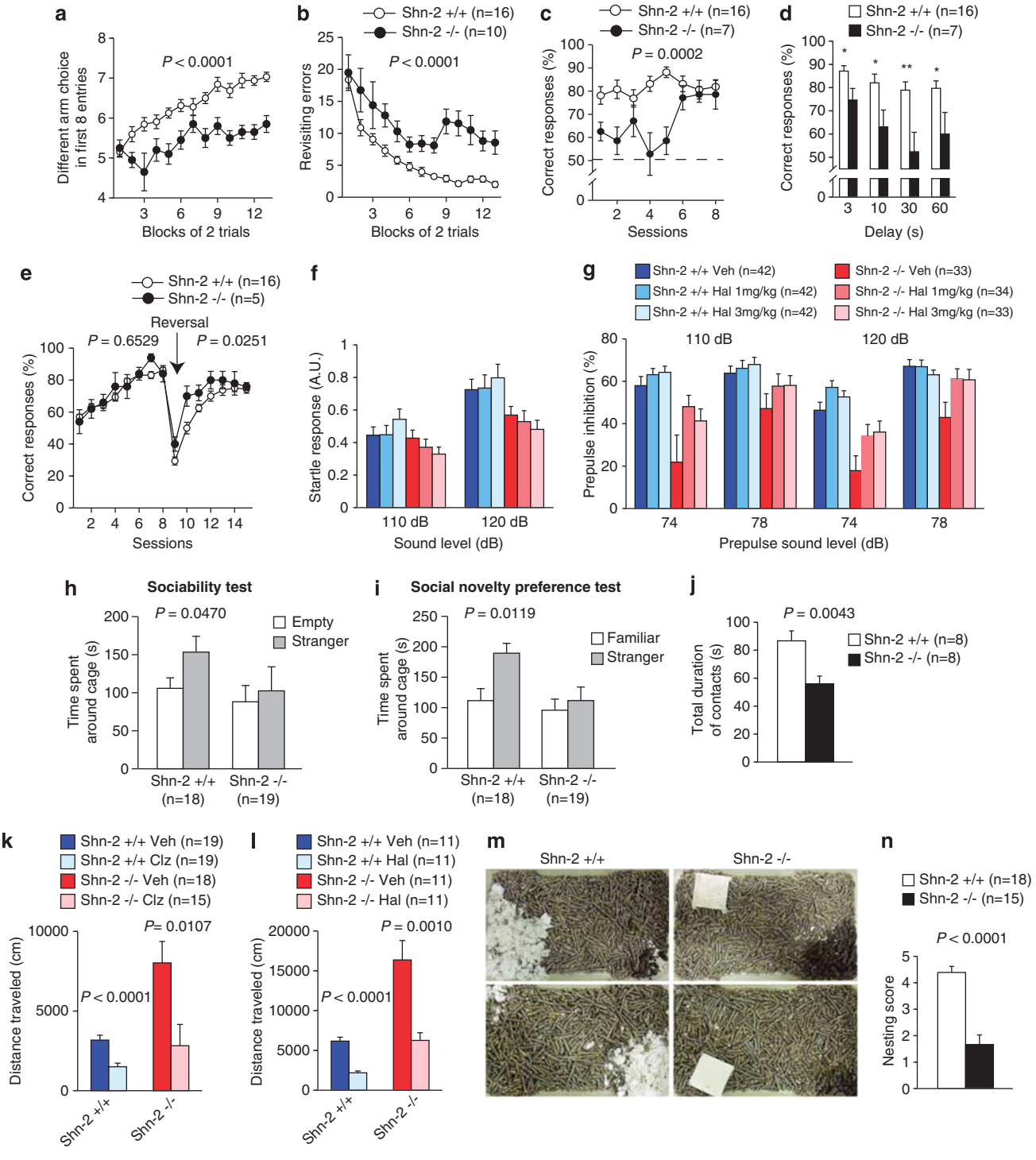

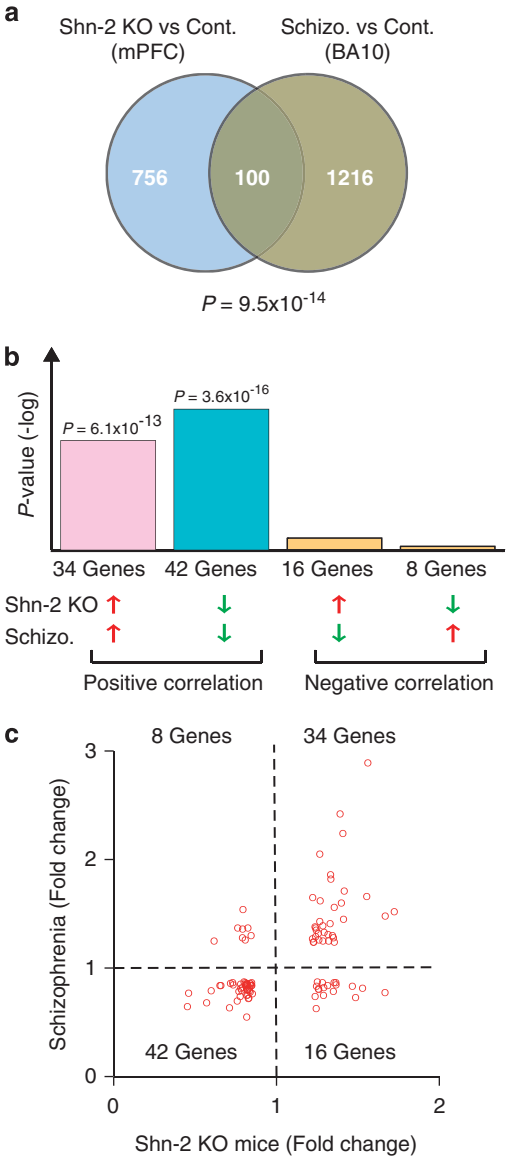

d

Gene symbol	Fold change	
	Shn−2 KO	Schizophrenia
Serpina3n	1.54	2.85
C1qb	1.37	2.38
C1qc	1.39	2.20
C10orf10	1.25	2.01
Rgs4	−1.25	−1.96
Ifitm2	1.31	1.82
C1qa	1.31	1.78
Myt1l	1.22	−1.70
Tac1	−1.44	−1.68
Cebpd	1.40	1.67
Frzb	−2.30	−1.65
Ifitm1	1.53	1.62
Tgfbr1	1.20	1.61
Frzb	−2.30	−1.59
Ddit4	1.25	1.58
Ifitm1	1.53	1.58
Cbln4	−1.81	−1.56
Tgm2	1.38	1.56
Mal2	−1.35	−1.52
Slc14a1	1.34	1.52
Mthfd2	−1.29	1.50
Gfap	1.70	1.48
Rgs4	−1.25	−1.48
D0H4S114	−1.24	−1.47
Fbxo9	−1.23	−1.46
Syn2	1.47	−1.45
Gadd45b	1.65	1.44
Gabra1	−1.32	−1.43
Chml	1.22	−1.43
Cebpb	1.39	1.41
Car10	1.27	−1.41
Rab3b	−1.25	−1.41
Tasp1	−1.24	−1.40
Hk2	1.25	1.39
RP11−35N6.1	−1.20	−1.38
Gng4	−2.26	−1.37
Ms4a6a	1.31	1.37
Klf10	1.65	−1.36
Fcgr3	1.27	1.35
Nrxn3	−1.22	−1.35

Figure 2 Comparison of gene expression profiles between Shn-2 KO mice and individuals with schizophrenia. (a) Venn diagram of genes differentially expressed in the medial prefrontal cortex (mPFC) of Shn-2 KO mice and Brodmann area (BA) 10 of postmortem schizophrenia brain (Schizo.). (b) *P*-values of overlap between Shn-2 KO mouse and schizophrenia data sets. (c) Scatter plot of gene expression fold change values in Shn-2 KO mice and schizophrenia. (d) Genes differentially expressed in both Shn-2 KO mice and schizophrenia. Red indicates gene upregulation and blue indicates downregulation in both Shn-2 KO mice and schizophrenia. The top 40 genes are included.

Figure 1 Schizophrenia-related behavioral abnormalities in Shn-2 KO mice. (a, b) In the spatial working memory version of the eight-arm radial maze, Shn-2 KO mice performed significantly worse with respect to the number of different arm choices in the first eight entries (genotype effect: $F_{1,24} = 62.104$, $P < 0.0001$) and made significantly more revisiting errors than controls (genotype effect: $F_{1,24} = 45.597$, $P < 0.0001$; genotype × trial block interaction: $F_{12,228} = 1.470$, $P = 0.1345$). (c) Mutant mice also showed poor working memory performance in the T-maze forced-alternation task (genotype effect: $F_{1,21} = 20.497$, $P = 0.0002$; genotype × session interaction: $F_{7,147} = 3.273$, $P = 0.0029$). (d) With increased delay, Shn-2 KO mice exhibited a lower correct percentage than controls (delay = 3, 10, 30, and 60 s; $P = 0.0010$, $P = 0.0047$, $P = 0.0083$, and $P = 0.0026$, respectively). (e) Shn-2 KO and wild-type mice were comparable in the left–right discrimination task (genotype effect: $F_{1,19} = 0.209$, $P = 0.6529$) and reversal learning (genotype effect: $F_{1,19} = 5.917$, $P = 0.0251$). (f) The amplitude of the acoustic startle response was not significantly different between genotypes (Shn-$2^{+/+}$, + Veh *vs* Shn-$2^{-/-}$, Veh, $F_{1,73} = 1.371$, $P = 0.2454$). (g) PPI of the acoustic startle response was impaired in Shn-2 KO mice (Shn-$2^{+/+}$, Veh *vs* Shn-$2^{-/-}$, Veh, 110 dB startle, $P = 0.0027$; 120 dB startle, $P = 0.0003$). Administration of haloperidol improved the PPI of Shn-$2^{-/-}$ mice (Shn-$2^{-/-}$, Veh *vs* Shn-$2^{-/-}$, 1 mg/kg Hal, 110 dB, $P = 0.0145$; 120 dB, $P = 0.0059$; Shn-$2^{-/-}$, Veh *vs* Shn-$2^{-/-}$, 3 mg/kg Hal, 120 dB, $P = 0.0044$). *Post hoc* Bonferroni's test after two-way repeated-measures ANOVA (level of significance was set at $P < 0.0167$). (h) Shn-2 KO mice display a lower level of social approach in the sociability test. (i) Shn-2 KO mice did not show social novelty preference. (j) Shn-2 KO mice displayed decreased social interaction in a novel environment (total contact duration: $F_{1,14} = 11.569$, $P = 0.0043$). (k) Administration of clozapine (1 mg/kg, i.p.) reversed hyperactivity in mutant mice (genotype effect: $P = 0.0012$, drug effect: $P = 0.0003$, genotype × drug interaction: $P = 0.0574$, Shn-$2^{-/-}$, Clz. *vs* Shn-$2^{+/+}$, Veh., $P = 0.4221$). (l) Administration of haloperidol (0.3 mg/kg, i.p.) also reduced hyperactivity in Shn-2 KO mice (genotype effect: $P < 0.0001$, drug effect: $P < 0.0001$, genotype × drug interaction: $P = 0.0275$, Shn-$2^{-/-}$, Hal. *vs* Shn-$2^{+/+}$, Veh., $P = 0.8957$). (m, n) Nest building was impaired in Shn-2 KO mice ($P < 0.0001$). Veh, Vehicle; Clz, Clozapine; Hal, Haloperidol.

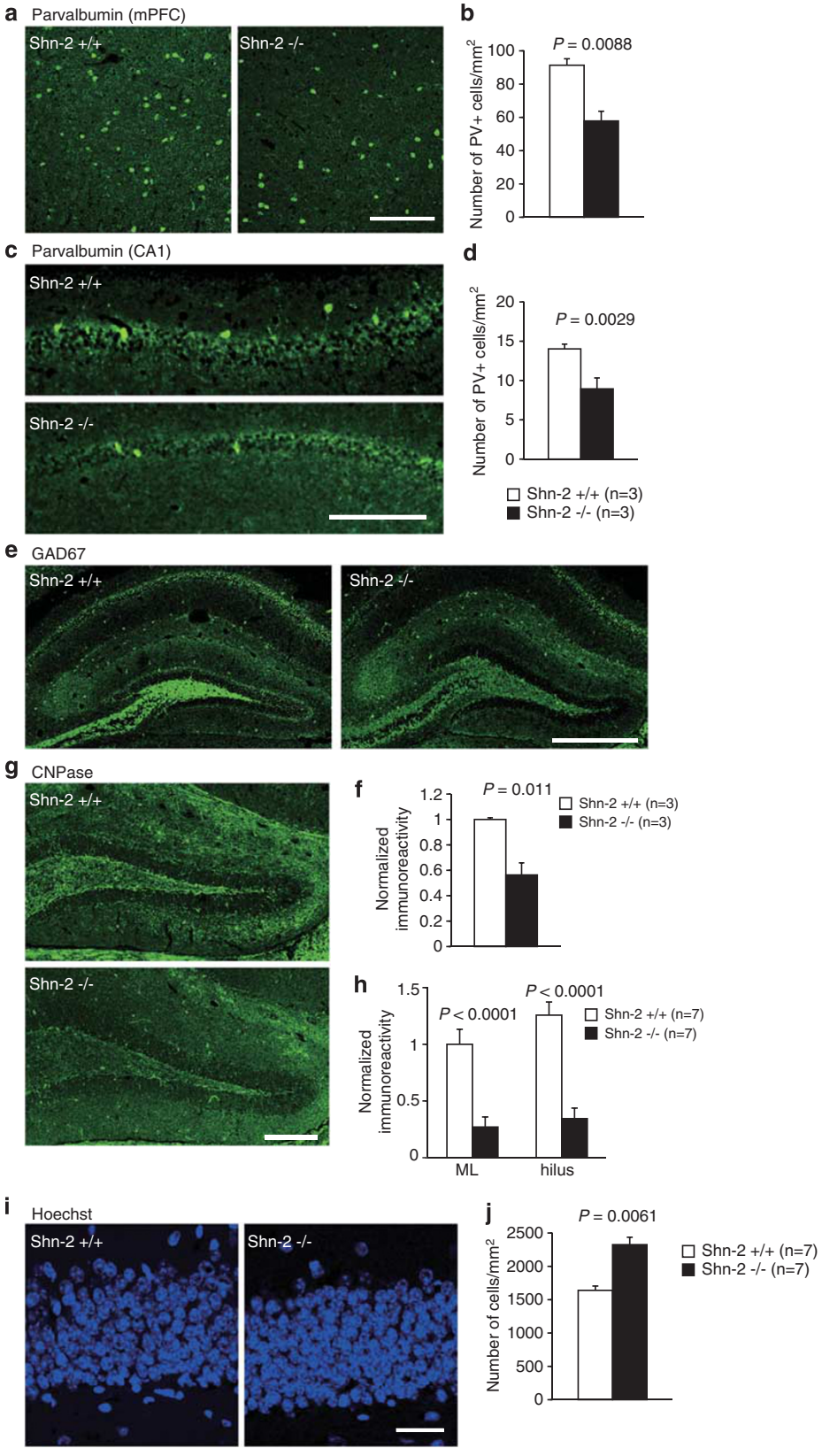

Figure 3 Schizophrenia-related alterations in the Shn-2 KO mouse brain. (a–d) The number of parvalbumin-positive cells is decreased in mPFC ($P = 0.0088$) (a, b) and CA1 ($P = 0.0029$) (c, d) of Shn-2 KO mice. (e, f) The expression of GAD67 in MFs of the hippocampus decreased in mutants ($P = 0.011$). (g, h) Reduced CNPase expression in the DG of Shn-2 KO mice compared with controls (molecular layer, $P < 0.0001$; hilus, $P < 0.0001$). (i, j) DG cell number was evaluated by staining cell nuclei with Hoechst dye. Cell-packing density was higher in Shn-2 KO mice ($P = 0.0061$) (j). GAD67, glutamic acid decarboxylase 67; CNPase, 2′,3-cyclic nucleotide 3′-phosphodiesterase; ML, molecular layer. Scale bars indicate 200 μm (a, c, g), 500 μm (e), 20 μm (i).

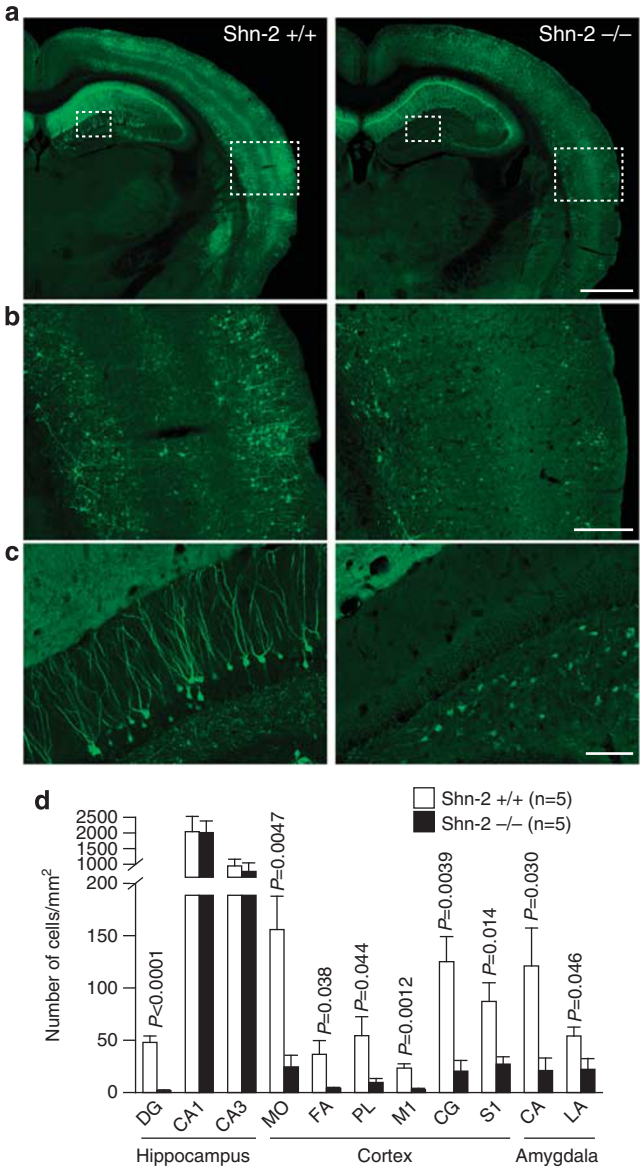

Figure 4 Reduced Arc induction in Shn-2 KO mice was observed after foot shocks in a novel environment. (a–c) Shn-2 KO mice were mated with transgenic mice expressing dVenus under the Arc promoter. Representative images of both genotypes are shown. (d) In Shn-2 KO mice, Arc-dVenus expression was greatly reduced in the DG and other regions of cortex and amygdala. Arc, activity-regulated cytoskeleton-associated protein. Scale bars indicate 1 mm (a), 250 μm (b), and 100 μm (c). MO, medial orbital cortex; FA, frontal association cortex; PL, prelimbic cortex; M1, primary motor cortex; CG, cingulate cortex; S1, somatosensory cortex; CA, central amygdaloid nucleus; LA, lateral amygdaloid nucleus.

Social withdrawal is a core symptom in schizophrenia according to the Diagnostic and Statistical Manual of Mental Disorders, Fourth Edition (DSM-IV). Mutant mice showed impaired sociability and novelty preference in Crawley's sociability and social novelty preference test (Figure 1h and i). Mutant mice also displayed decreased social interaction in the conventional social interaction test in a novel environment (Figure 1j; Supplementary Figure 2g and h). Consistent with a previous report (Takagi *et al*, 2006), Shn-2 KO mice displayed hyperactivity in the open field test (Supplementary Figure 2a) and in their home cages (Supplementary Figure 2b). Prior treatment with the antipsychotic haloperidol (0.3 mg/kg) or clozapine (1.0 mg/kg) decreased hyperactivity in Shn-2 KO mice to that of saline-treated control mice (Figure 1k and l). MK801, an NMDA antagonist that causes schizophrenia-like psychosis in humans, produced significantly higher levels of drug-stimulated motor activation in Shn-2 KO mice (Supplementary Figure 2j and k). The social activity of nest building in rodents is disrupted by the administration of psychomimetic agents (Schneider and Chenoweth, 1970). Nestlet shredding and nest building was severely impaired in Shn-2 KO mice (Figure 1m and n); Nestlets were left intact by ~80% of mutant mice, while all wild-type mice built nests within 24 h. Depression-like behavior of Shn-2 KO mice was increased in sucrose preference test (Figure 8n). In the Porsolt forced swim test, a reduction of immobility was observed in Shn-2 KO mice (Supplementary Figure 2f), possibly due to hyperactivity.

The improvement in PPI observed after haloperidol administration suggests that dopaminergic receptor signaling is altered in Shn-2 KO mice; therefore, we performed dopamine receptor binding assays to examine this. Because Shn-2 KO mice showed significantly reduced expression of D1 dopamine receptors in the DG (Supplementary Figure 3a), we examined the effects of D1 receptor activation on the phosphorylation status of the AMPA receptor, GluA1, at Ser845 (the PKA site) and extracellular signal-regulated kinase 2 (ERK2) at Thr202/Tyr204. The increases in GluA1 and ERK2 phosphorylation induced by SKF81297, a D1 receptor agonist, were greater in Shn-2 KO mice than in control mice (Supplementary Figure 3d–g). Normalization of phosphorylated GluA1 against total GluA1, which is decreased in Shn-2 KO mice (Supplementary Figure 3f, right), made these differences even greater (Supplementary Figure 3f, center). The increased levels of ERK2 phosphorylation observed in Shn-2 KO mice resulted from increased expression of ERK2 (Supplementary Figure 3g).

Shn-2 KO Mice Share Gene Expression Alterations with Postmortem Schizophrenia Brain

The medial prefrontal cortex (mPFC) (Goldman-Rakic, 1995) and DG (Gilbert and Kesner, 2006) have been suggested to play key roles in working memory, which is severely impaired in Shn-2 KO mice. Therefore, gene chip analysis was conducted to assess gene expression in the mPFC of Shn-2 KO mice. Significant up- or downregulation of 856 genes (980 probes) was observed in the mutants (P-value <0.05, fold-change <-1.2 or >1.2). We then compared the gene expression pattern in Shn-2 KO mice with those in patients with mental disorders from publicly available array data using the NextBio search engine. The highest degree of gene expression overlap was detected in postmortem schizophrenic and control tissue from the frontopolar part of the frontal cortex, Brodmann area 10 (BA10) (previously reported by Maycox *et al*, 2009; Figure 2a, $P=9.5\times10^{-14}$), with 100 genes altered in both Shn-2 KO mice and schizophrenia patients. Seventy-six genes out of those genes showed the same directional change in expression (Figure 2b–d) and, of these genes, 42 genes were downregulated ($P=3.6\times10^{-16}$) and 34 were upregulated ($P=6.1\times10^{-13}$). It is noteworthy that *HIVEP2* (*SHN2*) was significantly decreased in the schizophrenic

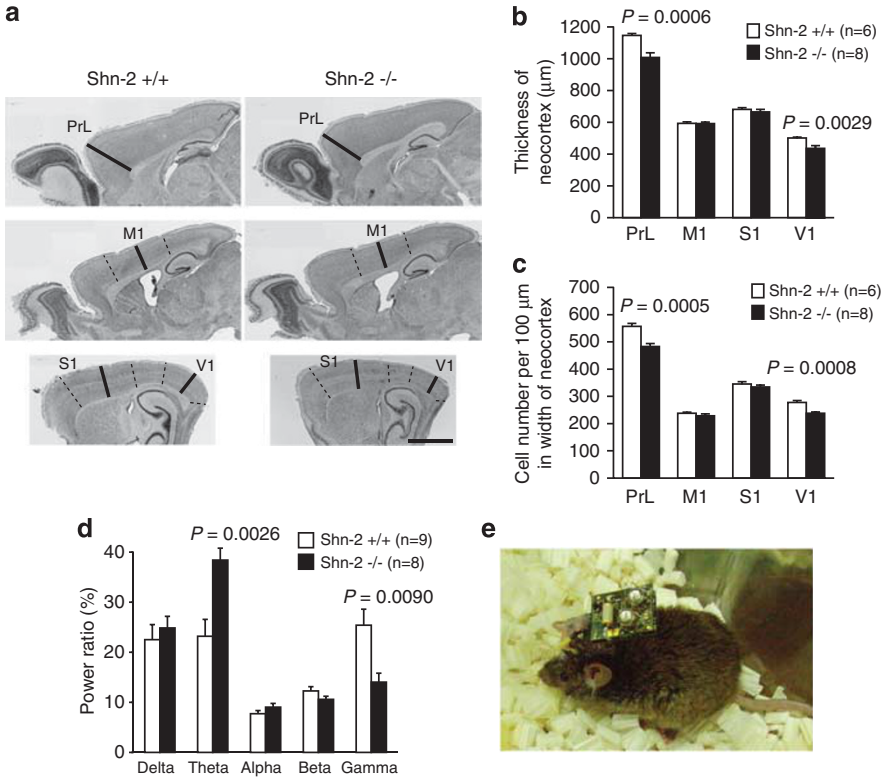

Figure 5 Abnormalities in the cortex of Shn-2 KO mice. (a, b) The cortex of Shn-2 KO mice was thinner than that of wild-type mice. Cortical cell density was also reduced in the prelimbic cortex (PrL) and primary visual cortex (V1) in Shn-2 KO mice (c). (d) Theta band power increased and gamma power decreased in Shn-2 KO mice. (e) A mouse with the Neurologger, a head-mounted EEG data logger device. M1, primary motor cortex; S1, primary somatosensory cortex. Scale bar indicates 1 mm (a).

BA10 (FC = −1.29, $P = 0.0009$) (Maycox *et al*, 2009). Within these groups, we noted a large number of genes previously implicated in schizophrenia or bipolar disorder (Supplementary Table 2). Eighty-nine of 100 genes showing significant similarities in terms of expression have been identified as being related to these disorders (Supplementary Table 2). Interestingly, six of the top 10 ranked genes were involved in inflammatory or immune responses.

Molecular Alterations in the Hippocampus of Shn-2 KO Mice

The granule cells of the hippocampal DG are compromised in schizophrenia (Altar *et al*, 2005; Tamminga *et al*, 2010). Because the DG is involved in spatial working memory (Gilbert and Kesner, 2006; Vann *et al*, 2000), deficits of which are cardinal features of schizophrenia, we analyzed the DG transcriptome of Shn-2 KO mice. Under the same criteria used for mPFC analysis, the expression of 1497 probes (1220 genes) was significantly up- or downregulated in the mutants (Supplementary Table 4). We also compared the DG transcriptome of Shn-2 KO mice to a study of laser-captured DG from human schizophrenia patients (Altar *et al*, 2005). *Calb1* (Shn-2 KO, FC = −5.36, $P = 0.001$; Schizo, FC = −1.82, $P = 0.001$), a marker of mature granule neurons, and *Rab33a* (Shn-2 KO, FC = −1.25, $P = 0.0023$; Schizo, FC = −1.96, $P = 0.0001$), a Ras-associated small GTPase, were both downregulated in the DG of Shn-2 KO mice and human schizophrenia patients.

We further analyzed the DG proteome in Shn-2 KO mice using two-dimensional difference gel electrophoresis (2D-DIGE) and found 116 proteins differentially expressed between mutant and control mice (Supplementary Table 5). When sorted by functional category, proteins in the same category were differentially expressed in both schizophrenia and Shn-2 KO mice. Supplementary Table 6 lists the genes and proteins with altered expression in both schizophrenic DG and Shn-2 KO brains (Altar *et al*, 2005) (including the DG (Supplementary Tables 4 and 5) and whole hippocampus (Supplementary Table 5)). Notably, the expression of aldo-keto reductase genes (particularly *AKR1A1* and *AKR1B1* and their mouse equivalents) was reduced in human patients and Shn-2 KO mice. Cytochrome-related genes *UQCRFS1* and *CYC1* were reduced in the DG of schizophrenia and the hippocampus of Shn-2 KO mice, as were genes encoding glucose phosphate isomerase, NADH dehydrogenase, phosphoglycerate-related molecules, proteasome, ubiquitin-related molecules, and syntaxins (Altar *et al*, 2005).

Immunohistochemistry of Shn-2 KO brains revealed several features observed in the postmortem brains of schizophrenia patients (Benes *et al*, 2007; Flynn *et al*, 2003; Reynolds and Beasley, 2001). Parvalbumin-positive neuronal number was decreased in the mPFC (Figure 3a and b) and hippocampal CA1 region (Figure 3c and d). The expression of glutamic acid decarboxylase 67 (GAD67) was lower in the mutant hippocampus (Figure 3e and f). The expression of 2′,3-cyclic nucleotide 3′-phosphodiesterase (CNPase), a marker for mature oligodendrocytes, was also

reduced (Figure 3g and h) and cell-packing density was higher in the DG of Shn-2 KO mice (Figure 3i and j).

Arc Induction Is Reduced in the Brains of Shn-2 KO Mice

Induction of the immediately early gene protein products has been used to assess neural activation. We crossed Shn-2 KO with transgenic mice expressing destabilized Venus (dVenus) under the control of the activity-regulated cytoskeletal-associated protein (Arc) promoter (Eguchi and Yamaguchi, 2009), allowing fluorescence-based visualization of Arc expression. We compared Arc-dVenus expression between Shn-2 KO and wild-type mice with the Arc-dVenus-positive background. To maximize Arc induction in the DG physiologically, mice received electrical shocks in a novel environment. Expression of Arc-dVenus in the DG 5 h after stimulation was dramatically reduced throughout the entire brain of Shn-2 KO mice (Figure 4), including amygdala (Figure 4a and d), sensory cortex (Figure 4b and d), motor cortex (Figure 4d), and PFC (Figure 4d). In the hippocampus of Shn-2 KO mice, dVenus expression was almost completely abolished in the DG (Figure 4c and d), with only minimal changes in CA regions. Reduced induction of Arc-dVenus was also observed 5 h after exposure to a novel environment without electrical shocks (Supplementary Figure 4).

Schizophrenia-Related Cortical Abnormalities in Shn-2 KO Mice

Shn-2 mutant mice display significantly thinner cortex and reduced cell density in the prelimbic and primary visual cortices (PrL and V1, respectively) when compared with wild-type mice (Figure 5a–c), which is consistent with observations in human patients (Pierri *et al*, 1999). Although the mutants demonstrated a reduction in cortical thickness, increased apoptosis was not appreciated in the brains of Shn-2 KO mice (Supplementary Figure 5). No obvious hallmarks of neurodegeneration, such as cell swelling, protein deposition, or nuclear condensation, were not found by electron microscopic analysis in the mutants (Supplementary Figure 6). The size of the whole brain, cerebrum, and cerebellum was not significantly different between genotypes (Supplementary Figure 7). Previous studies report increased low-frequency (Moran and Hong, 2011; Sponheim *et al*, 1994) and decreased high-frequency (Gallinat *et al*, 2004; Moran and Hong, 2011) energy in EEG studies of schizophrenia patients. We measured cortical EEG in freely moving mice using Neurologger spectral analysis technology (Figure 5e) and observed a significant increase of power in the theta band and decrease in the gamma band of Shn-2 KO mice compared with that in the controls (Figure 5d).

DG Maturation Deficits in Adult Shn-2 KO Mice

The behavioral abnormalities shown by Shn-2 KO mice resembled those observed in α-CaMKII$^{+/-}$ mice, which also show locomotor hyperactivity and severe working memory deficits (Yamasaki *et al*, 2008). To identify further similarities, we compared the hippocampal transcriptome patterns of both mouse models. Shn-2 KO mice and α-CaMKII$^{+/-}$ mice showed strikingly similar expression patterns (Figure 6a), with over 100 genes similarly altered. Moreover, the fold changes in differentially expressed genes were quite similar between strains (Figure 6a and b), indicating shared molecular pathophysiology between these mutants. In the hippocampus of α-CaMKII$^{+/-}$ mice, dentate granule cells fail to mature, characterized by increased expression of the immature-neuronal marker calretinin and decreased expression of the mature granule cell marker calbindin in the DG. Calbindin expression within the Shn-2 KO hippocampus is also dramatically decreased (Figure 6b and c) and was almost completely abolished in the DG (Figure 6c). As observed in α-CaMKII$^{+/-}$ mice, the number of cells positive for calretinin (Figure 6d) and PSA-NCAM (a late-progenitor and immature-neuron marker, Supplementary Figure 8) was increased dramatically in the Shn-2 KO DG. Collectively, these findings suggest that the number of immature neurons increases and that of mature neurons decreases, within the hippocampi of the two mutant mouse strains, that exhibited behavioral abnormalities related to schizophrenia.

Whole-cell recordings were made from granule cells in the DG. The cell membrane capacitance of Shn-2 KO mice decreased compared with that in controls (Figure 6e), indicating a smaller cell surface area. Granule cells in the DG of Shn-2 KO mice had a normal resting membrane potential (data not shown) and high input resistance (Figure 6f). In response to the current injection, Shn-2 KO cells demonstrated a lower current threshold for firing (Figure 6g), a short latency to the first spike (Figure 6h), and a decreased number of spikes during sustained depolarization (Figure 6i). Consistent with their immunohistological profile, granule cells in the mutant DG showed somatic electrophysiological features similar to those of immature granule cells (Schmidt-Hieber *et al*, 2004; Yamasaki *et al*, 2008).

We also examined synaptic transmission at the granule cell output, the mossy fiber (MF) synapse. The ratio of peak MF excitatory postsynaptic potential (EPSP) amplitude to fiber volley amplitude was increased in the mutant (Figure 6j), indicating significant augmentation of basal synaptic transmission. Strong frequency facilitation, an index of mature presynaptic function at the MF synapse (Kobayashi *et al*, 2010; Yamasaki *et al*, 2008), was greatly decreased in mutant mice (Figure 6k).

Evidence of CNS Inflammation within Shn-2 KO Mice

To characterize the molecular events happening in the Shn-2 KO mouse brain, correlation between Shn-2 KO gene expression data and thousands of publicly available array data sets were computed using the NextBio search engine using a rank-based algorithm (Sung *et al*, 2009). The top 300 biosets with the highest correlation scores with Shn-2 KO mice are categorized in Supplementary Table 7. Seven of the top 10 correlating biosets were categorized as 'aging.' Among the top 300 correlating biosets, 59 were categorized as aging, 18 as infection, 13 as injury, 12 as tumor, and 11 as neurodegeneration. Conspicuously, almost all biosets exhibiting gene expression changes similar to those in the brains of Shn-2 KO mice were related to inflammatory or

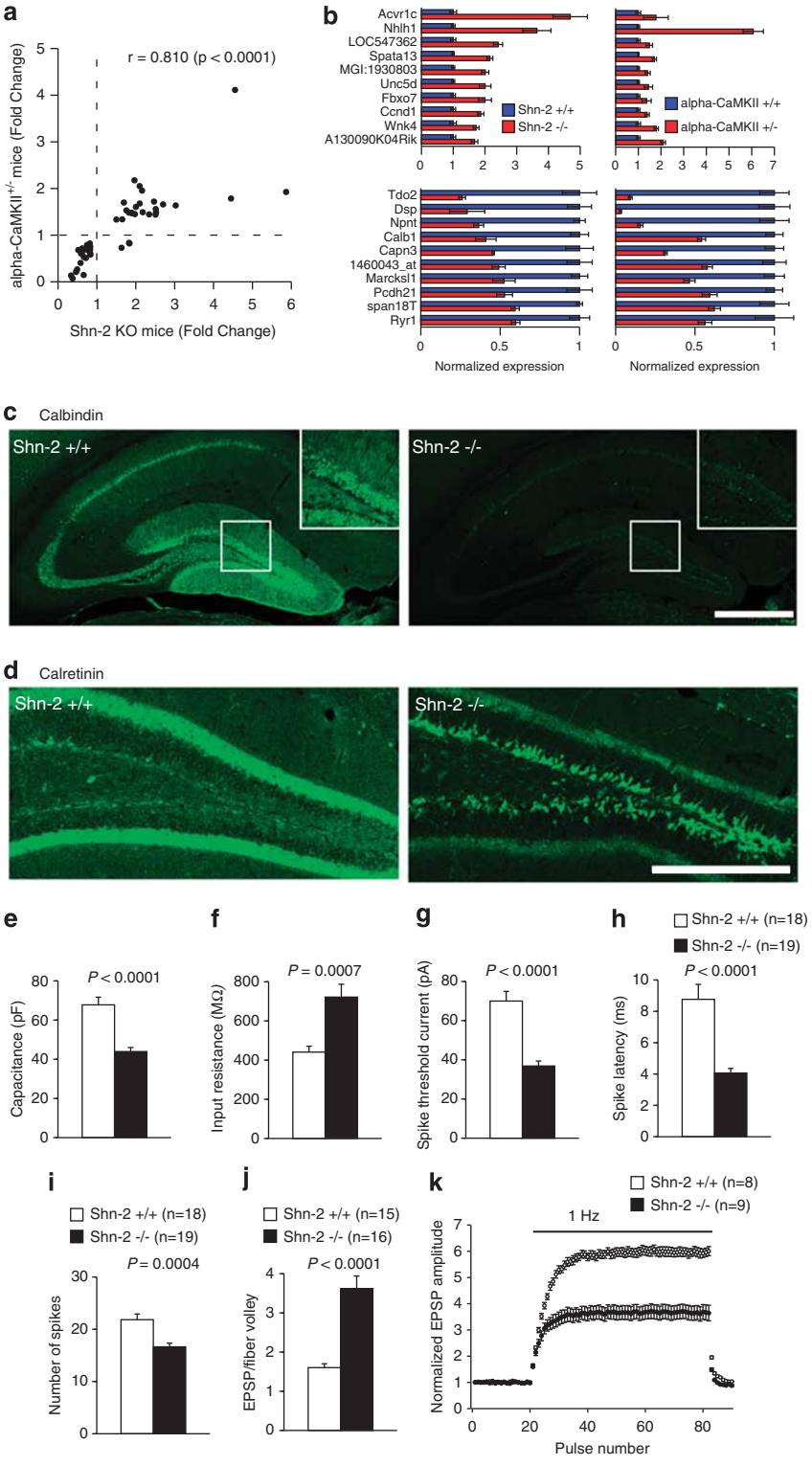

Figure 6 Dentate granule cells fail to mature in Shn-2 KO mice. (a) The hippocampal transcriptome pattern of Shn-2 KO mice was similar to that of α-CaMKII$^{+/-}$ mice, which also demonstrated maturation failure in the DG. Genes showing differential expression between genotypes at $P<0.005$ in both experiments were plotted. (b) Normalized gene expression of differentially expressed genes in Shn-2 KO and α-CaMKII$^{+/-}$ mice. The top 10 genes are indicated in the graphs. (c) The number of cells expressing the mature neuronal marker calbindin was decreased in Shn-2 KO mice. (d) The expression of the immature-neuronal marker calretinin was markedly increased. (e–k) Physiological properties of granule cells in the DG of Shn-2 KO mice and controls. Physiological features of DG neurons in the mutants were strikingly similar to those of immature DG neurons in normal rodents. Cell capacitance was small in the granule cells of Shn-2 KO mice (e, $P<0.0001$), whereas input resistance was high (f, $P=0.0007$), and the threshold current to induce spikes was low (g, $P<0.0001$). In the current injection (320 pA) experiments, the latency-to-burst spike was shorter (h, $P<0.0001$) and the number of spikes was lower (i, $P=0.0004$) compared with that in wild-type mice. (j) The efficacy of basal transmission at the MF synapse was increased in mutant mice ($P<0.0001$). The ratio of the peak EPSP amplitude to fiber volley amplitude is shown. (k) Shn-2 KO mice display greatly reduced frequency facilitation at 1 Hz (k, genotype effect: $P<0.0001$ at steady level). Scale bars indicate 500 μm (a), 250 μm (d).

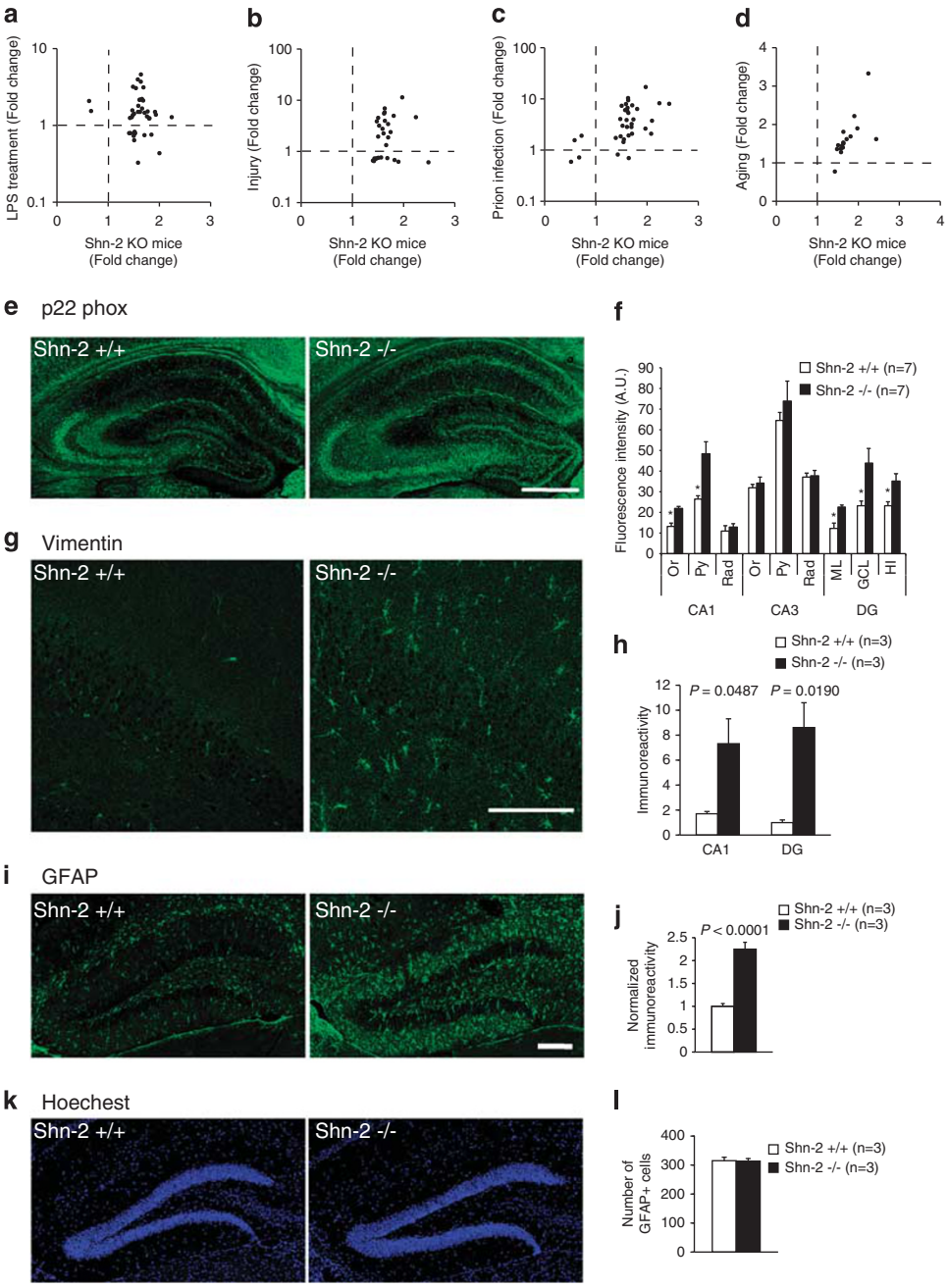

Figure 7 Inflammatory-like phenomena in the hippocampus of Shn-2 KO mice. (a–d) The hippocampal transcriptome pattern of Shn-2 KO mice was similar to the transcriptome data from LPS treatment (a), injury (b), prion infection (c), and aging (d). The Gene Expression Omnibus (GEO) accession numbers for the transcriptome data used for the graphs are GSE23182 (a, c), GSE5296 (b), and GSE13799 (d). Genes that showed differential expression between conditions at $P<0.005$ in Shn-2 KO mice and $P<0.025$ in LPS treatment were plotted in (a). Genes that showed differential expression between conditions at $P<0.005$ in both transcriptome data sets are plotted in (b–d). (e, f) The expression of p22 phox, a component of NADH/NADPH oxidase, was increased in the DG (ML, $P=0.027$; GCL, $P=0.048$; HI, $P=0.039$) and CA1 (Or, $P=0.011$; Py, $P=0.019$) of Shn-2 KO mice. (g, h) The expression of vimentin in the DG of mutants was higher than that of the controls. (i–k) The expression of GFAP was increased in the DG of Shn-2 KO mice. Although the area of GFAP-positive cells increased (j), the number of GFAP-positive cells remained unchanged (k, l), which was confirmed by Hoechest nuclear counterstaining. Or, oriens layer; Py, pyramidal cell layer; Rad, stratum radiatum; ML, molecular layer; GCL, granule cell layer; HI, hilus. Scale bars indicate 500 μm (e), 100 μm (g), and 200 μm (i).

immune responses. Similar gene perturbation patterns were found in the case of LPS treatment (Figure 7a, $P=5.6\times10^{-9}$), injury (Figure 7b, $P=5.7\times10^{-24}$), prion infection (Figure 7c, $P=1.0\times10^{-18}$) and aging (Figure 7d, $P=1.4\times10^{-26}$).

These results were particularly compelling, considering that Shn-2 is an endogenous inhibitor of NF-κB and that NF-κB is activated in Shn-2-deficient cells (Kimura *et al*, 2005). The expression of NF-κB-dependent genes such as *Ccnd1* (FC = 2.33, $P=0.0004$), *Hmox1* (FC = 1.69, $P=0.0215$), *Pdyn* (FC = 1.66, $P=0.0364$), *Ptgs2* (also known as *Cox2*, FC = 1.625, $P=0.0161$), *Traf1* (FC = 1.418, $P=0.0148$), and *Vim* (FC = 1.87, $P=0.0057$) was increased in the hippocampus of Shn-2 KO mice. Notably, genes

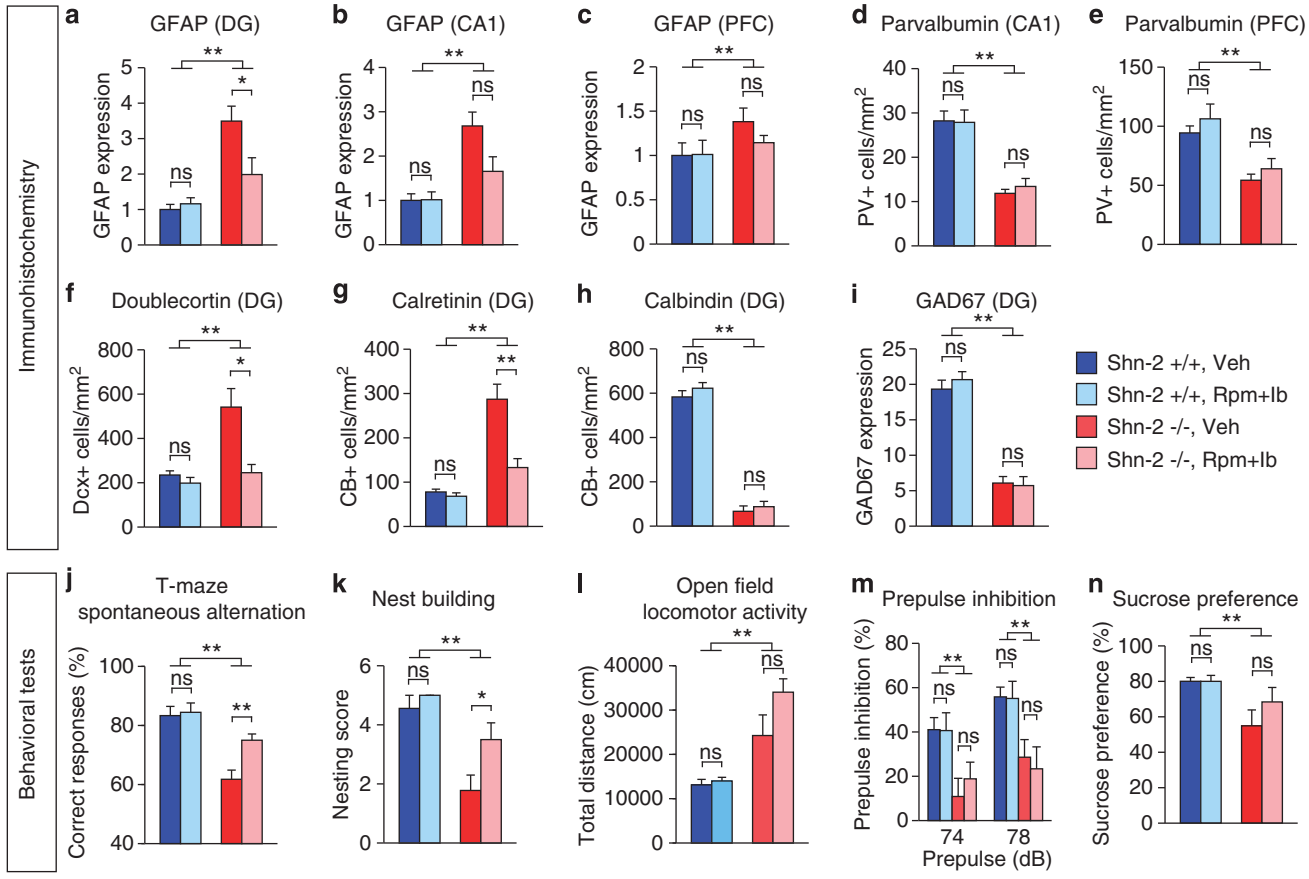

Figure 8 Anti-inflammatory treatment rescued neuronal and behavioral phenotypes of Shn-2 KO mice. Mice were chronically treated with rolipram (Rpm, 4 mg/kg) and ibuprofen (Ib, 400 p.p.m.) for 3 weeks. The treatment significantly decreased GFAP immunoreactivity in the DG of Shn-2 KO mice (a, genotype effect: $P<0.0001$; genotype × drug interaction: $P=0.014$; Shn-$2^{-/-}$, Veh *vs* Shn-$2^{-/-}$, Rpm + Ib, $P=0.0323$). There was a tendency of decrease in GFAP expression in the mutant CA1 (b, genotype effect: $P<0.0001$; genotype × drug interaction: $P=0.053$; Shn-$2^{-/-}$, Veh *vs* Shn-$2^{-/-}$, Rpm + Ib, $P=0.051$). The treatment did not reverse GFAP expression in the PFC of Shn-2 KO mice (c, genotype effect: $P=0.0717$; genotype × drug interaction: $P=0.3662$). The reductions of parvalbumin in CA1 (d, genotype effect: $P<0.0001$) or PFC (e, genotype effect: $P=0.0002$) were not rescued by the treatment. Increased expression of doublecortin (f, genotype effect: $P=0.0014$; genotype × drug interaction: $P=0.0014$; Shn-$2^{-/-}$, Veh *vs* Shn-$2^{-/-}$, Rpm + Ib, $P=0.0109$) and calretinin (g, genotype effect: $P<0.0001$; genotype × drug interaction: $P=0.0019$; Shn-$2^{-/-}$, Veh *vs* Shn-$2^{-/-}$, Rpm + Ib, $P=0.0028$) in the DG of Shn-2 KO mice were attenuated by the treatment, while decreased expressions of calbindin (h, genotype effect: $P<0.0001$) or GAD67 (i, genotype effect: $P<0.0001$) in the mutant DG were not rescued by the treatment. Working memory (j, genotype effect: $P<0.0001$; genotype × drug interaction: $P=0.0504$; Shn-$2^{-/-}$, Veh *vs* Shn-$2^{-/-}$, Rpm + Ib, $P=0.0042$) and nest-building behavior (k, genotype effect: $P<0.0001$; genotype × drug interaction: $P=0.1542$; Shn-$2^{-/-}$, Veh *vs* Shn-$2^{-/-}$, Rpm + Ib, $P=0.0407$) were significantly improved by the anti-inflammatory treatment in Shn-2 KO mice. On the other hand, hyperlocomotor activity (l), impaired PPI (m), or anhedonia in the sucrose preference test (n, genotype effect: $P=0.006$) were not improved. $n=5$–10 per group. Rpm, rolipram; Ib, ibuprofen; ns, not significant; $^{*}P<0.05$, $^{**}P<0.01$.

related to the inflammatory/immune response such as *Serpina3n*, *C1qa*, *C1qb*, *C1qc*, *Cyba*, *H2-Ab1*, *Tgfbr1*, *Cebpb*, *Ctsc*, *Lyn*, and *Tgfb1* were upregulated in the mPFC of Shn-2 KO mice and in postmortem brains of schizophrenia patients (Supplementary Table 2). We compared the gene expression patterns across various human brain disorders with that of Shn-2 KO mice (Supplementary Table 8). The biosets derived from schizophrenia patient groups showed the highest similarity to the bioset derived from Shn-2 KO mice ($P=9.50\times10^{-14}$), although the biosets derived from neurodegenerative disorders such as Alzheimer's disease and Parkinson's disease also showed significant similarities in expression to the biosets derived from Shn-2 KO mice. However, in spite of the similarities with neurodegenerative disorders, no obvious apoptosis or neurodegeneration was appreciated in the brains of Shn-2 KO mice (Supplementary Figures 5 and 6).

Next, immunohistochemistry was performed to detect molecular-level regulation by NF-κB. The expression of p22 phox NADPH oxidase, which causes inflammation via the release of reactive oxygen species (Manea *et al*, 2007), was increased in the DG and CA1 of Shn-2 KO mice (Figure 7e and f). Vimentin, an NF-κB-regulated (Kumar *et al*, 2004) intermediate filament protein found in immature astrocytes, was similarly increased (Figure 7g and h), as was glial fibrillary acidic protein (GFAP; Figure 7i and j). Although the area of GFAP-positive cells increased (Figure 7j), the number of GFAP-positive cells that was counted by staining with Hoechst was unchanged (Figure 7k and l). While astrocytes were activated in Shn-2 KO mice, microglias were not, as indicated by unaltered expression of the microglia marker, Iba1 (Supplementary Figure 10).

To assess whether inflammation plays any role in the behavioral abnormalities shown by Shn-2 KO mice, we

treated them with anti-inflammatory drugs (chronic administration of 4 mg/kg rolipram and fed chow containing 400 ppm ibuprofen) for 3 weeks. Treatment with anti-inflammatories reduced the number of activated astrocytes, which reflect inflammation within the hippocampi of the Shn-2 KO mice (Figure 8a and b), but did not affect the number of activated astrocytes in the PFC (Figure 8c). The decrease in parvalbumin (in the CA1 and PFC; Figure 8d and e), calbindin (in the DG; Figure 8h), and GAD67 (in the DG; Figure 8i) expression observed in the mutant mice was not rescued by treatment with anti-inflammatory drugs. Interestingly, the increase in the expression of doublecortin and calretinin in the DG of Shn-2 KO mice was reversed by treatment with anti-inflammatory drugs (Figure 8f and g). Moreover, working memory, as measured by the T-maze test and nest-building behavior were significantly improved in Shn-2 KO mice (Figure 8j and k). On the other hand, the increased locomotor activity observed in the open field test, the impaired PPI observed during the startle response, and the anhedonia in the sucrose preference test did not improve (Figure 8l–n). These results indicate that mild chronic inflammation occurring in the adult brain contributes to at least some of the behavioral deficits and cellular/molecular phenotypes seen in Shn-2 KO mice.

DISCUSSION

In the course of large-scale behavioral screening for mouse models of neuropsychiatric disorders, we discovered that Shn-2 KO mice display a series of schizophrenia-related behavioral abnormalities including severe working memory deficits, decreased social interaction, impaired nest-building behavior, and impaired PPI. We also identified conserved genetic and molecular phenotypes shared by both Shn-2 KO mice and postmortem brains of schizophrenia patients. Transcriptome patterns in the mPFC of Shn-2 KO mice and the PFC of schizophrenia patients are strikingly similar. Additionally, Shn-2 KO mice possessed an immature DG (iDG) phenotype that has also been identified in α-CaMKII$^{+/-}$ mice, which display behavioral abnormalities similar to those observed in Shn-2 KO mice (Yamasaki *et al*, 2008). Supplementary Table 11 summarizes the phenotypes of the Shn-2 KO mice and the abnormalities associated with schizophrenia. Since the disorder is composed of a heterogeneous population, even an 'ideal' animal model of schizophrenia, if any, will not necessarily exhibit the abnormalities observed in all schizophrenia-relevant phenotypes (Powell and Miyakawa, 2006). However, Shn-2 KO mice exhibit an unusually high number of similarities compared with other existing animal models of schizophrenia.

Of the top 20 biogroups whose genes that showed significant overlap with those whose expression was changed in postmortem schizophrenia brains (Maycox *et al*, 2009), 14 were involved in immune responses. Most of the genes within these biogroups were upregulated (Supplementary Table 3), suggesting that inflammation or immune activation occurs in the brains of both schizophrenic patients and Shn-2 KO mice. The overall hippocampal transcriptome pattern of Shn-2 KO mice exhibited similarities to patterns identified in a number of inflammatory conditions, including aging, injury, prion infection, and adjuvant treatment (Supplementary Table 7), in which NF-κB signaling is activated. We found significant increases in the expression level of many complement genes and MHC/HLA genes in Shn-2 KO mice (Supplementary Table 9). Notably, C1qa, C1qb, C1qc, H2-Aa (HLA-DQA1), and H2-Ab1 (HLA-DQB1) were upregulated in the brains of both Shn-2 KO mice and patients with schizophrenia. C1q is proposed to act as a spreading 'punishment signals' that bind to weaker synapses resulting in their physical removal (Fourgeaud and Boulanger, 2007). In this regard, it is of interest to note that the expression of the genes related to 'synaptic transmission,' the dysregulation of which is also thought to be involved in schizophrenia (Mirnics *et al*, 2001; Stephan *et al*, 2006), tended to be downregulated in the brains of both Shn-2 KO mice and schizophrenic patients (Supplementary Table 3). Upregulation of C1q genes could be a potential interface between inflammation and synaptic dysfunctions. Interestingly, the levels of majority of pro-inflammatory cytokines, including those that play a role in acute inflammation (eg, IL-1 and TNF-α), were unchanged in the brains of Shn-2 KO mice and schizophrenic patients (Supplementary Table 9). These data indicate the atypical nature of inflammation happening in the brains of Shn-2 KO mice and, potentially, in those of schizophrenic patients. The precise manner in which these genes are altered is likely to be complex and remains to be determined. A number of SNPs in the MHC region associated with schizophrenia (Purcell *et al*, 2009; Shi *et al*, 2009, 2011; Stefansson *et al*, 2009; Yue *et al*, 2011). Supplementary Table 10 lists the SNPs located in, or close to, NF-κB-binding sites that may be associated with susceptibility to schizophrenia. Some of the genes surrounding these SNPs are dysregulated in the postmortem brains of schizophrenic patients and/or the PFC of Shn-2 KO mice. Abnormal transcription of these genes may be induced by dysregulated NF-κB signaling pathways, without any deficiency or mutation in Shn-2 itself.

Astrocytes were activated in the hippocampus of Shn-2 KO mice, while microglias were largely inactive. In humans, type-I and type-II immune responses are defined by the respective cytokines activated. The type-I response mainly promotes cell-mediated immune responses against intracellular pathogens with the activation of Th1 CD4+ cells and microglias (Muller and Schwarz, 2006). The type-II immune response is largely directed against extracellular pathogens in which Th2 CD4+ cells and astrocytes are activated (Muller and Schwarz, 2006). This atypical pattern of inflammation is also observed in schizophrenia patients, who demonstrate attenuated type-I immune responses and activated type-II immune responses (Muller and Schwarz, 2006). This so-called 'Th2 slant' can be observed in the CNS, with astrocytes reflecting the type-2 immune response and microglias reflecting the type-1 immune response (Muller and Schwarz, 2006), in schizophrenia patients as well as Shn-2 KO mice (Kimura *et al*, 2007). Accordingly, the astrocyte activation observed in Shn-2 KO and schizophrenia may result from type-2 immune activation. Microglial activation is also reported in schizophrenia, but only within a small percentage of postmortem brains, possibly as a side effect of medication (Bayer *et al*, 1999; Muller and Schwarz, 2006). Pharmacological experiments indicate that deficits in working memory and nest-building behavior

could be rescued by treatment with anti-inflammatory drugs, which also reduced GFAP expression, a widely used inflammation marker, in the brains of Shn-2 KO mice. These results suggest that mild chronic inflammation caused by deficiency of Shn-2 underlies at least some behavioral abnormalities related to schizophrenia.

The well-established role of inflammation in the etiology of schizophrenia is often referred to as the inflammation hypothesis (Keshavan *et al*, 2011; Patterson, 2009; Muller and Schwarz, 2006; Nawa and Takei, 2006). The link between prenatal infection and schizophrenia was first identified in an epidemiological study demonstrating increased schizophrenia risk in the offspring of women exposed to influenza during pregnancy (Muller and Schwarz, 2006). Several other infectious factors have also been implicated in the pathogenesis of schizophrenia (Muller and Schwarz, 2006), suggesting that the disease may result from maternal immune response to infection. To this end, prenatal Poly I:C treatment, viral infection, and LPS treatment are used as rodent models of schizophrenia (Patterson, 2009; Nawa and Takei, 2006). To the best of our knowledge, the Shn-2 KO mouse is the first animal model of schizophrenia with multiple inflammatory-like phenomena arising from a single gene knockout.

In schizophrenia patients, the number of parvalbumin-positive neurons decreases in the cortex (Reynolds and Beasley, 2001) and hippocampus (Zhang and Reynolds, 2002), which could cause a deficit in the density of certain GABAergic neuronal subtypes. Inflammatory responses evoked by neonatal LPS treatment were reported to induce a reduction in parvalbumin-expressing neurons in the rat hippocampus (Jenkins *et al*, 2009). Overexpression of IL-6 (Heyser *et al*, 1997), which is secreted during type-II immune responses, also reduces the number of parvalbumin-positive neurons (Muller and Schwarz, 2006). Similarly, a previous study reported that IL-6 mediates age-related loss of critical parvalbumin-expressing GABAergic interneurons through increased neuronal NADPH oxidase-derived superoxide production (Dugan *et al*, 2009). Consistently, IL-6 was increased in the T cells (Kimura *et al*, 2005) of Shn-2 KO mice.

Attenuation of molecular markers for schizophrenia may also result from inflammation. Ketamine exposure, which has been used as a model of schizophrenia based on NMDA hypofunction, reduces parvalbumin and GAD67 expression through increased NADPH oxidase and p22 phox, suggesting inflammation (Behrens *et al*, 2007). Schizophrenia patients express lower levels of GABAergic neuron-expressed GAD67 in the stratum oriens of CA2/3 (Benes *et al*, 2007), suggesting the possibility that these deficits lead to neuronal GABA hypofunction. We also observed several potential deficits in key oligodendrocyte markers, including decreases in CNPase and myelin basic protein (MBP). Decreased CNPase protein levels have been reported in schizophrenia (Flynn *et al*, 2003). Similarly, MBP mRNA levels, a major constituent of the myelin sheath of oligodendrocytes and Schwann cells, were decreased in the mPFC of Shn-2 KO mice (Supplementary Table 2). Inflammatory cytokines and autoimmune components are suggested to damage oligodendrocytes (Calzà *et al*, 1998). Thus, CNPase and MBP downregulation suggests a possible inflammation-related abnormality in Shn-2 KO oligodendrocytes, consistent with the so-called 'oligodendrocyte hypothesis' of schizophrenia.

Adult but not juvenile Shn-2 KO mice display an abnormally thin cortex, which is also observed in schizophrenia patients (Pierri *et al*, 1999). Cortical thickness is reduced by aging (Salat *et al*, 2004), which in turn is associated with inflammation. Gene expression patterns in the cortex of Shn-2 KO mice significantly overlapped ($P = 1.1 \times 10^{-17}$) with a previous data set comparing whole-brain gene expression patterns in young (8-week-old) and aged (2-year-old) mice. These data suggest that similar mechanisms may underlie the reduction of cortical thickness in aging and Shn-2 KO mice.

In addition to anatomical abnormalities, the Shn-2 KO mouse cortex displays physiological alterations. Upon cortical EEG analysis, mutant mice displayed increases in slow waves and decreases in fast waves, both of which are observed in schizophrenia patients (Gallinat *et al*, 2004; Moran and Hong, 2011; Sponheim *et al*, 1994). Computational model study suggested that downregulation of parvalbumin neurons reduced gamma oscillation (Volman *et al*, 2011), agreeing with our observations of Shn-2 KO mice. Immaturity of DG in Shn-2 KO mice may underlie their abnormal theta rhythm in their cortex, considering the close functional relationship between hippocampus and mPFC as demonstrated by their coordinated activity (Jones and Wilson, 2005).

Induction of Arc transcription after receiving foot shocks in a novel environment was generally reduced in almost all regions of the Shn-2 KO brain. Despite this near-ubiquitous reduction of Arc, we observed comparable Arc expression in the CA1 and CA3 regions of the hippocampus in Shn-2 KO and wild-type mice. The relatively higher Arc expression in these regions suggests that CA areas in Shn-2 KO may be comparatively more active than other brain regions. This idea is consistent with increased glutamate level in the hippocampus of Shn-2 KO mice (Supplementary Figure 11). In stark contrast to control mice, virtually no Arc induction was observed in the Shn-2 KO mouse DG, which displays significant immaturity. The gene expression pattern associated with iDG-like phenomena has been observed in fluoxetine-treated (Kobayashi *et al*, 2010) and α-CaMKII$^{+/-}$ mice, whose DG also shows dramatically reduced expressions of immediately early genes, such as c-Fos and/or Arc (Kobayashi *et al*, 2010; Yamasaki *et al*, 2008; Matsuo *et al*, 2009). Although such an extreme phenotype may not be common in schizophrenic patients, this finding is particularly interesting for several reasons. Reduced expression of Arc mRNA in the PFC (Maycox *et al*, 2009) and DG (Talbot *et al*, 2011) of postmortem schizophrenia brains has been reported. A recent *de novo* copy-number variation (CNV) analysis suggests that Arc protein complexes play a role in the pathogenesis of schizophrenia (Kirov *et al*, 2012). Specifically, *de novo* CNVs found in schizophrenic patients are significantly enriched in the postsynaptic density (PSD) proteome; these include Arc protein complexes. It was recently shown that, upon synaptic activation, Arc is translocated to neighboring inactive synapses. This may potentially increase the signal-to-noise ratio at plastic synapses (Okuno *et al*, 2012). Loss or dysfunction of the Arc complex may impair the synaptic input into neurons and subsequently cause cognitive

deficits in both schizophrenic patients and animal models of the disease. Interestingly, DG granule cells of mice treated with chronic fluoxetine produced repeated spikes but generated little immediate-early gene expression (Kobayashi *et al*, 2010). Thus, altered signal transmission likely reduces Arc induction.

An increasing number of schizophrenia mouse models show impairment in hippocampus-dependent tasks. Mouse mutants of disrupted-in-schizophrenia 1 (DISC1) (Li *et al*, 2007) and dysbindin-1 (Takao *et al*, 2008), which are widely accepted models of schizophrenia, show deficits in spatial working memory, which is a DG-dependent function. DISC1 is highly expressed in the DG during adulthood (Meyer and Morris, 2008), and mice lacking a C-terminal portion of DISC1 show morphological abnormalities in the DG and spatial working memory deficits (Li *et al*, 2007). Dysbindin-1 is expressed at high levels in the DG and MF. In schizophrenia patients, the reduction of dysbindin-1 is relatively restricted to the DG and MF terminal field (Talbot *et al*, 2004). Sdy mutant mice lacking the dysbindin-1 gene show working memory impairment (Takao *et al*, 2008) and reduced frequency facilitation in hippocampal MF-CA3 synapse (Kobayashi *et al*, 2011). α-CaMKII$^{+/-}$ mice display severe working memory deficits and have well-defined features of iDG (Matsuo *et al*, 2009; Yamasaki *et al*, 2008). We recently reported that calretinin, an immature-neuronal marker, is significantly upregulated in the DG of postmortem brains in human schizophrenia/bipolar patients (Walton *et al*, 2012). Thus, the iDG phenotype may represent an additional 'endophenotype' that is shared by human schizophrenic patients and some schizophrenia mouse models. Since iDG neurons can produce spikes with lower current injection compared with mature neurons, the hippocampus harboring iDG may have a lower activation threshold. In the Shn-2 KO mouse brain, hippocampal hyperactivation was suggested by the fact that Arc induction in CA1 and CA3 was comparable to wild-type levels, while other regions exhibited an overall reduction. These observations suggest that the Shn-2 KO mouse hippocampus may be activated to a higher degree than that of controls. There was a marked reduction in strong frequency facilitation at the MF-CA3 synapse, a form of short-term plasticity, in Shn-2 KO mice. In agreement with this, the number of synapses per MF terminal was lower in postmortem schizophrenia brain tissue than in healthy control tissue (Tamminga *et al*, 2010). Reduced frequency facilitation was also reported in DISC1 mutant mice (Kvajo *et al*, 2011). These studies and our results collectively suggest that schizophrenia patients and some animal models of the disease may have hippocampal abnormalities, including iDG phenotype.

Pre-weaned animals showed no significant differences in calbindin (Supplementary Figure 9a and b), calretinin (Supplementary Figure 9e and f), p22 phox (Supplementary Figure 9i and j), or GFAP (Supplementary Figure 9m and n) expression between genotypes. The expression of p22 phox in older (1-month-old) mutant animals was increased (Supplementary Figure 9k and l) whereas that of GFAP was not significantly different (Supplementary Figure 9o and p). Calbindin expression was decreased (Supplementary Figure 9c and d), and calretinin was increased (Supplementary Figure 9g and h) in the DG of 1-month-old Shn-2 KO mice compared to that of wild-type mice, indicating an iDG phenotype. These observation suggest that neither astrocyte activation, increase of reactive oxygen species production, nor 'iDG' phenotype are present in the brain of Shn-2 KO mice before weaning, and that these phenotypes emerged during postnatal development, which is consistent with the fact that most cases of schizophrenia appear in late adolescence or early adulthood.

Together, our results demonstrate that Shn-2 deficiency caused atypical inflammation and associated hippocampal and cortical abnormalities, imbalance of GABA-glutamate, and abnormal myelination. These alterations, as a whole, may bring about behavioral abnormalities related to schizophrenia in Shn-2-deficient mice. Thus, the Shn-2 KO mouse displays good face and concept validity, and may be useful in elucidating the pathogenesis and pathophysiology of schizophrenia.

DISCLOSURE

Noah M Walton and Mitsuyuki Matsumoto are employees of the Astellas Research Institute of America LLC, a subsidiary of Astellas Pharma Inc. The other authors declare no conflict of interest.

ACKNOWLEDGEMENTS

This work was supported by KAKENHI (24111546, 20023017, 18023022, 17025023, 22380078) from the Ministry of Education, Culture, Sports, Science and Technology (MEXT) of Japan, Promotion of Fundamental Studies in Health Sciences of the National Institute of Biomedical Innovation (NIBIO), Neuroinformatics Japan Center (NIJC), and by grants from CREST & BIRD of Japan Science and Technology Agency (JST).

REFERENCES

Altar CA, Jurata LW, Charles V, Lemire A, Liu P, Bukhman Y *et al* (2005). Deficient hippocampal neuron expression of proteasome, ubiquitin, and mitochondrial genes in multiple schizophrenia cohorts. *Biol Psychiatry* **58**: 85–96.

Bayer TA, Buslei R, Havas L, Falkai P (1999). Evidence for activation of microglia in patients with psychiatric illnesses. *Neurosci Lett* **271**: 126–128.

Behrens MM, Ali SS, Dao DN, Lucero J, Shekhtman G, Quick KL *et al* (2007). Ketamine-induced loss of phenotype of fast-spiking interneurons is mediated by NADPH-oxidase. *Science* **318**: 1645–1647.

Benes FM, Lim B, Matzilevich D, Walsh JP, Subburaju S, Minns M (2007). Regulation of the GABA cell phenotype in hippocampus of schizophrenics and bipolars. *Proc Natl Acad Sci USA* **104**: 10164–10169.

Braff DL, Freedman R, Schork NJ, Gottesman II (2007). Deconstructing schizophrenia: an overview of the use of endophenotypes in order to understand a complex disorder. *Schizophr Bull* **33**: 21–32.

Calzà L, Giardino L, Pozza M, Bettelli C, Micera A, Aloe L (1998). Proliferation and phenotype regulation in the subventricular zone during experimental allergic encephalomyelitis: *in vivo* evidence of a role for nerve growth factor. *Proc Natl Acad Sci* **95**: 3209–3214.

Dugan LL, Ali SS, Shekhtman G, Roberts AJ, Lucero J, Quick KL *et al* (2009). IL-6 mediated degeneration of forebrain

GABAergic interneurons and cognitive impairment in aged mice through activation of neuronal NADPH oxidase. *PLoS One* **4**: e5518.

Eguchi M, Yamaguchi S (2009). *In vivo* and *in vitro* visualization of gene expression dynamics over extensive areas of the brain. *Neuroimage* **44**: 1274–1283.

Flynn SW, Lang DJ, Mackay AL, Goghari V, Vavasour IM, Whittall KP *et al* (2003). Abnormalities of myelination in schizophrenia detected *in vivo* with MRI, and post-mortem with analysis of oligodendrocyte proteins. *Mol Psychiatry* **8**: 811–820.

Fourgeaud L, Boulanger LM (2007). Synapse remodeling, compliments of the complement system. *Cell* **131**: 1034–1036.

Fukuda S, Yamasaki Y, Iwaki T, Kawasaki H, Akieda S, Fukuchi N *et al* (2002). Characterization of the biological functions of a transcription factor, c-myc intron binding protein 1 (MIBP1). *J Biochem* **131**: 349–357.

Gallinat J, Winterer G, Herrmann CS, Senkowski D (2004). Reduced oscillatory gamma-band responses in unmedicated schizophrenic patients indicate impaired frontal network processing. *Clin Neurophysiol* **115**: 1863–1874.

Gilbert PE, Kesner RP (2006). The role of the dorsal CA3 hippocampal subregion in spatial working memory and pattern separation. *Behav Brain Res* **169**: 142–149.

Goldman-Rakic PS (1995). Cellular basis of working memory. *Neuron* **14**: 477–485.

Hagihara H, Toyama K, Yamasaki N, Miyakawa T (2009). Dissection of hippocampal dentate gyrus from adult mouse. *J Vis Exp* **33**: e1543.

Heyser CJ, Masliah E, Samimi A, Campbell IL, Gold LH (1997). Progressive decline in avoidance learning paralleled by inflammatory neurodegeneration in transgenic mice expressing interleukin 6 in the brain. *Proc Natl Acad Sci USA* **94**: 1500–1505.

Jenkins TA, Harte MK, Stenson G, Reynolds GP (2009). Neonatal lipopolysaccharide induces pathological changes in parvalbumin immunoreactivity in the hippocampus of the rat. *Behav Brain Res* **205**: 355–359.

Jones MW, Wilson MA (2005). Theta rhythms coordinate hippocampal–prefrontal interactions in a spatial memory task. *PLoS Biol* **3**: e402.

Kalkstein S, Hurford I, Gur RC (2010). Neurocognition in schizophrenia. *Curr Top Behav Neurosci* **4**: 373–390.

Keshavan MS, Nasrallah HA, Tandon R (2011). Schizophrenia, 'Just the Facts' 6. Moving ahead with the schizophrenia concept: from the elephant to the mouse. *Schizophr Res* **127**: 3–13.

Kimura MY, Hosokawa H, Yamashita M, Hasegawa A, Iwamura C, Watarai H *et al* (2005). Regulation of T helper type 2 cell differentiation by murine Schnurri-2. *J Exp Med* **201**: 397–408.

Kimura MY, Iwamura C, Suzuki A, Miki T, Hasegawa A, Sugaya K *et al* (2007). Schnurri-2 controls memory Th1 and Th2 cell numbers *in vivo*. *J Immunol* **178**: 4926–4936.

Kirov G, Pocklington AJ, Holmans P, Ivanov D, Ikeda M, Ruderfer D *et al* (2012). *De novo* CNV analysis implicates specific abnormalities of postsynaptic signalling complexes in the pathogenesis of schizophrenia. *Mol Psychiatry* **17**: 142–153.

Kobayashi K, Ikeda Y, Sakai A, Yamasaki N, Haneda E, Miyakawa T *et al* (2010). Reversal of hippocampal neuronal maturation by serotonergic antidepressants. *Proc Natl Acad Sci USA* **107**: 8434–8439.

Kobayashi K, Umeda-Yano S, Yamamori H, Takeda M, Suzuki H, Hashimoto R (2011). Correlated alterations in serotonergic and dopaminergic modulations at the hippocampal mossy fiber synapse in mice lacking dysbindin. *PLoS One* **6**: e18113.

Kumar A, Takada Y, Boriek AM, Aggarwal BB (2004). Nuclear factor-kappaB: its role in health and disease. *J Mol Med* **82**: 434–448.

Kurosawa G, Sumitomo M, Akahori Y, Matsuda K, Muramatsu C, Takasaki A *et al* (2009). Methods for comprehensive identification of membrane proteins recognized by a large number of monoclonal antibodies. *J Immunol Methods* **351**: 1–12.

Kvajo M, McKellar H, Drew LJ, Lepagnol-Bestel A-M, Xiao L, Levy RJ *et al* (2011). Altered axonal targeting and short-term plasticity in the hippocampus of Disc1 mutant mice. *Proc Natl Acad Sci* **108**: E1349–E1358.

Li W, Zhou Y, Jentsch JD, Brown RAM, Tian X, Ehninger D *et al* (2007). Specific developmental disruption of disrupted-in-schizophrenia-1 function results in schizophrenia-related phenotypes in mice. *Proc Natl Acad Sci USA* **104**: 18280–18285.

Manea A, Manea SA, Gafencu AV, Raicu M (2007). Regulation of NADPH oxidase subunit p22(phox) by NF-kB in human aortic smooth muscle cells. *Arch Physiol Biochem* **113**: 163–172.

Matsuo N, Yamasaki N, Ohira K, Takao K, Toyama K, Eguchi M *et al* (2009). Neural activity changes underlying the working memory deficit in alpha-CaMKII heterozygous knockout mice. *Front Behav Neurosci* **3**: 20.

Maycox PR, Kelly F, Taylor A, Bates S, Reid J, Logendra R *et al* (2009). Analysis of gene expression in two large schizophrenia cohorts identifies multiple changes associated with nerve terminal function. *Mol Psychiatry* **14**: 1083–1094.

Meyer KD, Morris JA (2008). Immunohistochemical analysis of Disc1 expression in the developing and adult hippocampus. *Gene Expression Patterns* **8**: 494–501.

Mirnics K, Middleton FA, Lewis DA, Levitt P (2001). Analysis of complex brain disorders with gene expression microarrays: schizophrenia as a disease of the synapse. *Trends Neurosci* **24**: 479–486.

Miyakawa T, Leiter LM, Gerber DJ, Gainetdinov RR, Sotnikova TD, Zeng H *et al* (2003). Conditional calcineurin knockout mice exhibit multiple abnormal behaviors related to schizophrenia. *Proc Natl Acad Sci USA* **100**: 8987–8992.

Moran LV, Hong LE (2011). High *vs* low frequency neural oscillations in schizophrenia. *Schizophr Bull* **37**: 659–663.

Muller N, Schwarz M (2006). Schizophrenia as an inflammation-mediated dysbalance of glutamatergic neurotransmission. *Neurotox Res* **10**: 131–148.

Nawa H, Takei N (2006). Recent progress in animal modeling of immune inflammatory processes in schizophrenia: implication of specific cytokines. *Neurosci Res* **56**: 2–13.

Okuno H, Akashi K, Ishii Y, Yagishita-Kyo N, Suzuki K, Nonaka M *et al* (2012). Inverse synaptic tagging of inactive synapses via dynamic interaction of Arc/Arg3.1 with CaMKIIβ. *Cell* **149**: 886–898.

Patterson PH (2009). Immune involvement in schizophrenia and autism: etiology, pathology and animal models. *Behav Brain Res* **204**: 313–321.

Pierri JN, Chaudry AS, Woo TU, Lewis DA (1999). Alterations in chandelier neuron axon terminals in the prefrontal cortex of schizophrenic subjects. *Am J Psychiatry* **156**: 1709–1719.

Powell CM, Miyakawa T (2006). Schizophrenia-relevant behavioral testing in rodent models: a uniquely human disorder? *Biol Psychiatry* **59**: 1198–1207.

Purcell SM, Wray NR, Stone JL, Visscher PM, O'Donovan MC, Sullivan PF *et al* (2009). Common polygenic variation contributes to risk of schizophrenia and bipolar disorder. *Nature* **460**: 748–752.

Reynolds GP, Beasley CL (2001). GABAergic neuronal subtypes in the human frontal cortex–development and deficits in schizophrenia. *J Chem Neuroanat* **22**: 95–100.

Salat DH, Buckner RL, Snyder AZ, Greve DN, Desikan RSR, Busa E *et al* (2004). Thinning of the cerebral cortex in aging. *Cerebral Cortex* **14**: 721–730.

Schmidt-Hieber C, Jonas P, Bischofberger J (2004). Enhanced synaptic plasticity in newly generated granule cells of the adult hippocampus. *Nature* **429**: 184–187.

Schneider CW, Chenoweth MB (1970). Effects of hallucinogenic and other drugs on the nest-building behaviour of mice. *Nature* **225**: 1262–1263.

Shatz CJ (2009). MHC class I: an unexpected role in neuronal plasticity. *Neuron* **64**: 40–45.
Shi J, Levinson DF, Duan J, Sanders AR, Zheng Y, Pe'er I *et al* (2009). Common variants on chromosome 6p22.1 are associated with schizophrenia. *Nature* **460**: 753–757.
Shi Y, Li Z, Xu Q, Wang T, Li T, Shen J *et al* (2011). Common variants on 8p12 and 1q24.2 confer risk of schizophrenia. *Nat Genet* **43**: 1224–1227.
Sponheim SR, Clementz BA, Iacono WG, Beiser M (1994). Resting EEG in first-episode and chronic schizophrenia. *Psychophysiology* **31**: 37–43.
Stefansson H, Ophoff RA, Steinberg S, Andreassen OA, Cichon S, Rujescu D *et al* (2009). Common variants conferring risk of schizophrenia. *Nature* **460**: 744–747.
Stephan KE, Baldeweg T, Friston KJ (2006). Synaptic plasticity and dysconnection in schizophrenia. *Biol Psychiatry* **59**: 929–939.
Sung W-K, Lu Y, Lee CWH, Zhang D, Ronaghi M, Lee CGL (2009). Deregulated direct targets of the hepatitis B virus (HBV) protein, HBx, identified through chromatin immunoprecipitation and expression microarray profiling. *J Biol Chem* **284**: 21941–21954.
Swerdlow NR, Light GA, Cadenhead KS, Sprock J, Hsieh MH, Braff DL (2006). Startle gating deficits in a large cohort of patients with schizophrenia: relationship to medications, symptoms, neurocognition, and level of function. *Arch Gen Psychiatry* **63**: 1325–1335.
Takagi T, Jin W, Taya K, Watanabe G, Mori K, Ishii S (2006). Schnurri-2 mutant mice are hypersensitive to stress and hyperactive. *Brain Res* **1108**: 88–97.
Takao K, Toyama K, Nakanishi K, Hattori S, Takamura H, Takeda M *et al* (2008). Impaired long-term memory retention and working memory in sdy mutant mice with a deletion in Dtnbp1, a susceptibility gene for schizophrenia. *Mol Brain* **1**: 11.
Talbot K, Eidem WL, Tinsley CL, Benson MA, Thompson EW, Smith RJ *et al* (2004). Dysbindin-1 is reduced in intrinsic, glutamatergic terminals of the hippocampal formation in schizophrenia. *J Clin Invest* **113**: 1353–1363.
Talbot K, Ong W, Ho M, Samoyedny AJ, Arnold SE (2011). Hippocampal formation expression of the immediate early gene Arc/Arg3.1 is reduced in dysbindin-1 null protein mice and schizophrenia cases. *Society Neurosci* **368**: 08.
Tamminga CA, Stan AD, Wagner AD (2010). The hippocampal formation in schizophrenia. *Am J Psychiatry* **167**: 1178–1193.
Vann SD, Brown MW, Erichsen JT, Aggleton JP (2000). Fos imaging reveals differential patterns of hippocampal and parahippocampal subfield activation in rats in response to different spatial memory tests. *J Neurosci* **20**: 2711–2718.
Volman V, Behrens MM, Sejnowski TJ (2011). Downregulation of parvalbumin at cortical GABA synapses reduces network gamma oscillatory activity. *J Neurosci* **31**: 18137–18148.
Walton NM, Zhou Y, Kogan JH, Shin R, Webster M, Gross AK *et al* (2012). Detection of an immature dentate gyrus feature in human schizophrenia/bipolar patients. *Transl Psychiatry* **2**: e135.
Yamasaki N, Maekawa M, Kobayashi K, Kajii Y, Maeda J, Soma M *et al* (2008). Alpha-CaMKII deficiency causes immature dentate gyrus, a novel candidate endophenotype of psychiatric disorders. *Mol Brain* **1**: 6.
Yue W-H, Wang H-F, Sun L-D, Tang F-L, Liu Z-H, Zhang H-X *et al* (2011). Genome-wide association study identifies a susceptibility locus for schizophrenia in Han Chinese at 11p11.2. *Nat Genet* **43**: 1228–1231.
Zhang ZJ, Reynolds GP (2002). A selective decrease in the relative density of parvalbumin-immunoreactive neurons in the hippocampus in schizophrenia. *Schizophr Res* **55**: 1–10.

Supplementary Information accompanies the paper on the Neuropsychopharmacology website (http://www.nature.com/npp)